

# Fusing Iris Colour and Texture information for fast iris recognition on mobile devices

Chiara Galdi  
EURECOM  
Sophia Antipolis, France  
Email: chiara.galdi@eurecom.fr

Jean-Luc Dugelay  
EURECOM  
Sophia Antipolis, France  
Email: jean-luc.dugelay@eurecom.fr

**Abstract**—A novel approach for fast iris recognition on mobile devices is presented in this paper. Its key features are: (i) the use of a combination of classifiers exploiting the iris colour and texture information; (ii) its limited computational time, particularly suitable for fast identity checking on mobile devices; (iii) the high parallelism of the code, making this approach also appropriate for identity verification on large database. The proposed method has been submitted to the Mobile Iris CHallenge Evaluation II. The test set employed for the contest evaluation is made available on the contest web page. The latter has been used to assess the performance of the proposed method in terms of Recognition Rate (RR) and Area Under Receiver Operating Characteristic Curve (AUC).

## I. INTRODUCTION

Performing biometric recognition, and in particular iris recognition, on smartphones is a very challenging issue but also a trending topic nowadays. In recent years, researchers have addressed many problems related to iris recognition on mobile devices, usually originating from the use of visible light sources and a number of noise factors occurring during the acquisition of the iris image, such as out-of-focus images, specular or diffuse reflections, eyelid or eyelash occlusions, low resolution images, etc. [1], [2]. These studies have produced many valuable findings on specific aspects of iris recognition on mobile devices, such as novel techniques for iris segmentation exploiting the Watershed transform [5], or for secure home banking based on user iris verification [3], [4].

Since 2015, the first smartphones integrating user identity verification based on the iris have entered the market<sup>1</sup>. These devices employ embedded near-infrared (NIR) light sources, directing a beam of near-infrared light at the person's eye [6]. This kind of illumination is used because it is invisible to human eyes and allows to light eyes up without annoying the users. On the other hand, since the light emitted by the near-IR LED is invisible, it enters the eye pretty much unobstructed<sup>2</sup>. The manufacturers ensure that the use of NIR LED “is completely safe to use and there are no health implications associated with the technology” and users are recommended to do not stare at the NIR LED light and “In addition, the

light will automatically switch off if the device detects that your eyes are too close or exposed to the IR LED for more than nine seconds”<sup>3</sup>.

Nevertheless, developing solutions for accurate iris recognition in visible light is of paramount importance, taking into consideration the fact that there are many application scenarios in which NIR illumination is not available or applicable. For example for continuous re-identification, i.e. when the system continuously verifies the user identity, in which case the user cannot be constantly exposed to NIR light, since the effects of a prolonged exposure to NIR light are still uncertain. Another example scenario in which NIR illumination cannot be available is for forensic, i.e. the process of analyzing images or videos to verify the identity of a person.

In this paper, we present a novel approach for iris recognition particularly designed for iris recognition on smartphones and presented to the MICHE II - Mobile Iris CHallenge Evaluation Part II held in 2016<sup>4</sup>. The algorithm is based on the combination of three feature extractors, each of which describes a different characteristic of the iris: an iris colour descriptor, an iris texture descriptor, and an iris colour spots (hereinafter “clusters”) descriptor.

The key features of the proposed method are: the use of the colour information (only available when using visible light illumination), the suitability for noisy iris recognition, the limited computational time, and the high parallelization.

The performances obtained, AUC of 0.98 in the best case, are very interesting, although far from being perfect, considering that the presented method only leverage on the iris information (the periocular area is not taken into account).

The remainder of the paper is organized as follows: in section II, the multi-classifier algorithm is described; in section III the experimental results are presented and section IV concludes the paper.

## II. COLOUR AND TEXTURE FEATURE BASED MULTI-CLASSIFIER

The presented algorithm is made up of three descriptors, namely the colour descriptor, the texture descriptor and the

<sup>1</sup><http://webcup.com/list-of-all-eye-scanner-iris-retina-recognition-smartphones/>

<sup>2</sup>[http://www.phonearena.com/news/Here-is-how-the-Galaxy-Note-7-iris-scanner-works\\_id82854](http://www.phonearena.com/news/Here-is-how-the-Galaxy-Note-7-iris-scanner-works_id82854)

<sup>3</sup><https://news.samsung.com/global/everything-you-need-to-know-about-the-galaxy-note7s-iris-scanner>

<sup>4</sup>[http://biplab.unisa.it/MICHE\\_Contest\\_ICPR2016/index.php](http://biplab.unisa.it/MICHE_Contest_ICPR2016/index.php)

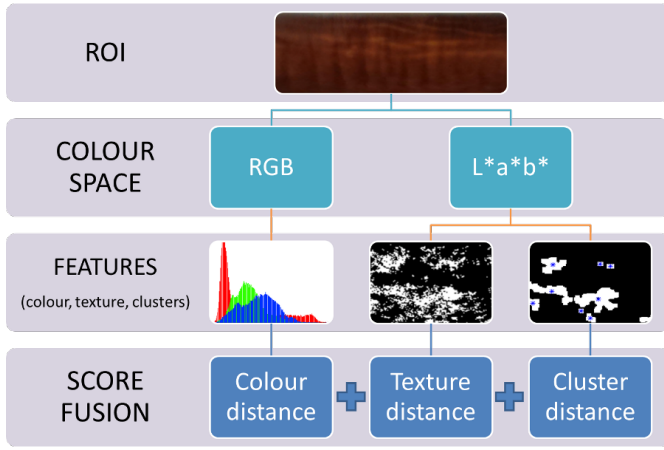


Fig. 1. Algorithm flow chart.

cluster descriptor. In figure 1, a flow chart describing the proposed approach is given.

### A. Colour descriptor

The colour descriptor is based on a technique designed for image retrieval in image database. The colour distribution is analysed and used to retrieve images similar to the query image. The Euclidean distance between the colour histograms of the two images to compare is computed as follows:

$$d(h, g) = \sqrt{\sum_A \sum_B \sum_C (h(a, b, c), g(a, b, c))^2}$$

where  $h$  and  $g$  represent the two colour histograms and  $(a, b, c)$  represent the three colour channels,  $rgb$  in our case.

Given two iris images to be compared, each picture is first split in small blocks and for each pair of corresponding blocks from the two images, the colour distance is computed. The minimum colour distance obtained is the final score returned by the colour descriptor.

### B. Texture descriptor

The texture descriptor is based on the computation of the MinkowskiBouligand dimension, also known as box-counting dimension. The box-counting dimension of a set  $S$  is defined as follows:

$$dim_{box}(S) := \lim_{\varepsilon \rightarrow 0} \frac{\log N(\varepsilon)}{\log(\frac{1}{\varepsilon})}$$

where  $N(\varepsilon)$  is the number of boxes of side length  $\varepsilon$  required to cover the set  $S$ .

The input image is first divided into several layers obtained by a decomposition process illustrated in the following. Each layer  $l_i$ , where  $i = 1, 2, \dots, N$  and  $N$  is the number of layers, is further divided in small blocks  $b_{i,j}$ , where  $i$  is the corresponding layer and  $j = 1, 2, \dots, M$  and  $M$  is the number of blocks. For each block  $b_{i,j}$ , the corresponding box-counting dimension  $d_{b_{i,j}}$  is computed. Finally, the distances  $d_{b_{i,j}}$  are concatenated in a feature vector.

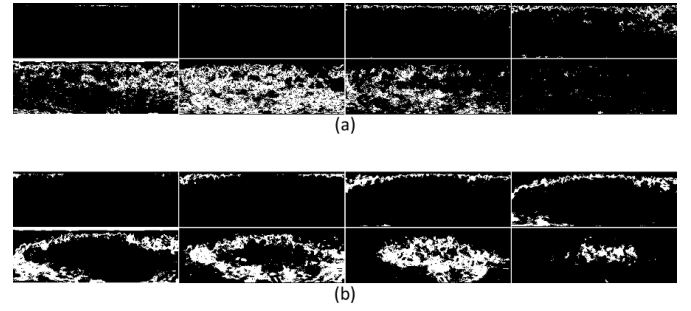


Fig. 2. Iris image multi-layer decomposition: a) the 8 layers obtained from the colour channel  $a^*$ ; b) the 8 layers obtained from the colour channel  $b^*$ .

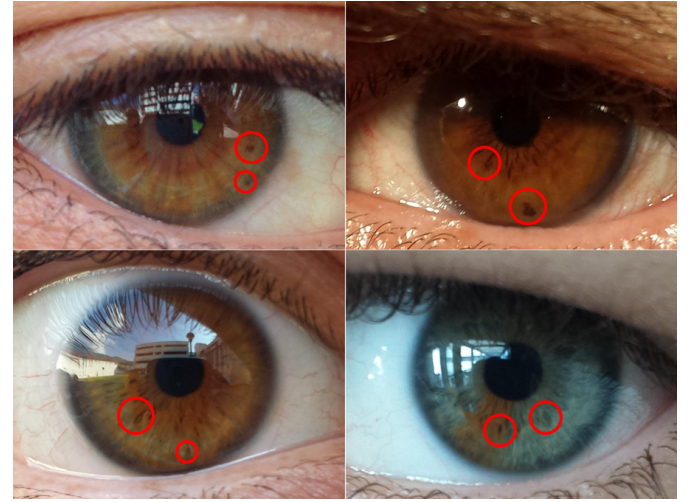


Fig. 3. Iris colour spots examples.

Feature vectors coming from different iris images are compared through the Euclidean distance.

1) *Multi-layer iris image decomposition*: The input iris image is first projected in the CIE 1976  $L^*a^*b^*$  colour space, where  $L^*$  is the lightness dimension and  $a^*$  and  $b^*$  are the colour-opponent dimensions.

Only the colour dimensions are further processed since the lightness information is more likely to be different also among images of the same iris, e.g. if the lighting conditions have changed between the acquisitions of the same user.

For each colour channel ( $a^*$  and  $b^*$ ) the values are first normalized between 0 and 255, then the resulting grey values are divided in 8 intervals of size 32 ( $32 \cdot 8 = 256$ ), i.e. 8 layers (images) are obtained from each colour channel, where the first layer contains the pixels with values in  $[0, 31]$ , the second in  $[32, 63]$ , ..., and the last in  $[224, 255]$ . For each layer, the value of the pixels belonging to the corresponding interval are set to 1 while all the others are set to 0. A sample iris image multi-layer decomposition is given in figure 2.

### C. Cluster descriptor

With "clusters" we mean the small colour spots that often characterize the human iris. This idea comes from the observation that humans leverage on these small spots (if the iris

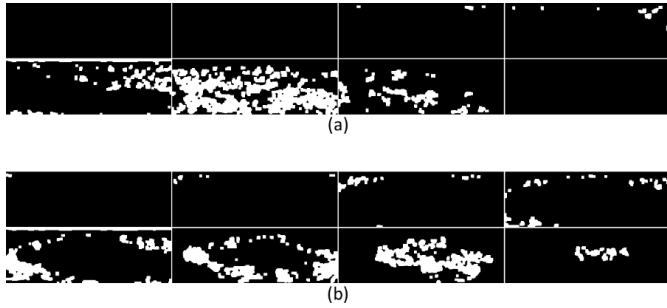


Fig. 4. Iris clusters representation on the 16 layers originating from the image decomposition. a) clusters on the  $a^*$  colour channel layers; b) clusters detected on the  $b^*$  channel layers.

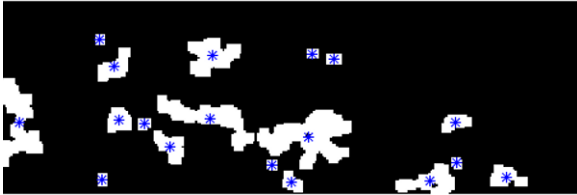


Fig. 5. Cluster centroids visualization.

images are in grey scale or if the colour of the observed irises is similar) to determine if the observed images are of the same iris or not. In figure 3, it is possible to observe some of these colour spots. The two irises in the first column, for example, are very similar in terms of colour, but the darker colour spots (circled in red in the image) allow the observer to distinguish them.

To have a representation of these clusters, the input iris image is first processed by the multi-layer decomposition previously illustrated (section II-B1). On each layer, a closing morphological operation, followed by an opening, is performed. The resulting clusters are the connected components (white pixels) showed in the example in figure 4.

For each cluster, the following properties are computed (by using the MATLAB function *regionprops*):

- Centroid coordinates;
- Orientation;
- Eccentricity.

Their corresponding values are concatenated in a feature vector. For each layer, a list of cluster feature vectors is obtained. When two iris images have to be compared, for each pair of corresponding layers, the two lists of cluster feature vectors are matched following the all-versus-all scheme and the average distance of the best matching pairs (i.e. the pair of clusters with minimum distance) is computed. Thus, a distance value for each pair of corresponding layers is obtained, the final score is given by averaging them. In figure 4, the centroids are plotted on the corresponding clusters of a given layer.

#### D. Classifiers fusion

The fusion of the three classifiers is performed by a weighted sum, where the weights are set to a value propor-



Fig. 6. Colour normalization: in the first row some original pictures from the MICHE database are shown; the second row illustrates the same pictures after colour normalization.

tional to the performance of the corresponding classifier and the sum of the weights is 1.

### III. EXPERIMENTAL RESULTS

In this section some implementation details and the experimental results obtained in the MICHE II contest are presented.

#### A. Data preprocessing

The database employed for the MICHE II challenge is the MICHE database, a large set of iris images captured by different mobile devices in different and unconstrained conditions [7]. The images contained in the MICHE DB are affected by many different noise factors, in particular we addressed: (i) the different colour appearance due to varying illumination conditions and different capturing device characteristics; (ii) the eyelid occlusion, that hides a large part of the iris features.

In order to solve problem (i), a colour normalization technique is applied, namely the *grey world* normalization. The grey world normalization makes the assumption that changes in the lighting spectrum can be modelled by three constant factors applied to the red, green and blue channels of colour [8]. The results of the colour normalization on some sample MICHE DB pictures are illustrated in figure 6.

Problem (ii) is addressed by selecting a part of the iris that is more likely to be not occluded by eyelids. The original iris images are first processed by the Haindl and Krupicka algorithm for iris segmentation [9], made available to all MICHE II participants. The resulting iris image is a mapping of the iris from polar to Cartesian coordinates, i.e. a rectangular image of size  $100 \times 600$  pixels. In these pictures, the eyelid occlusions are mostly located on the two image sides. For this reason, only the central part of the iris is selected, obtaining a region of interest (ROI) of  $100 \times 300$  pixels (see figure 7).

#### B. Parallelization

It is worth noticing that in several phases of the proposed method, the image is split in small blocks or decomposed in a

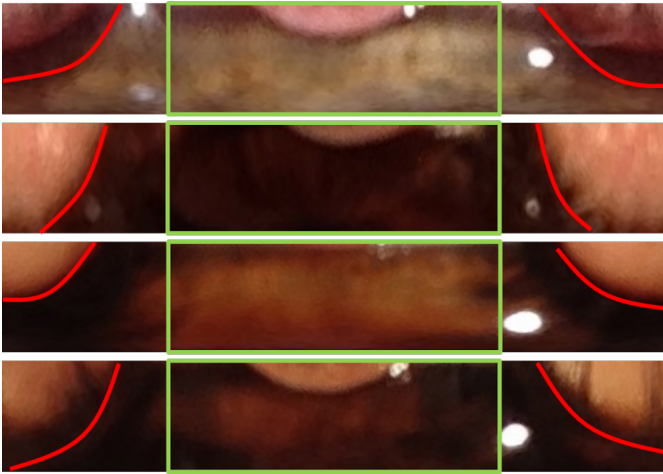


Fig. 7. ROI selection on 4 sample images of the MICHE DB: in green, the ROI selected from the iris image; in red, the eyelid occlusions.

number of layers. The operations applied on each block/layer are independent and thus the computation can be parallelized.

For experimental reproducibility, some implementation details are given: (i) ROI size =  $100 \times 300$  pixels; (ii) the block size in the colour descriptor is of  $50 \times 75$  pixels; (iii) the number of layers obtained by the image decomposition is 16, 8 from the  $a^*$  channel and 8 from the  $b^*$ ; (iv) the block size in the texture descriptor is of  $25 \times 75$  pixels.

### C. Performance evaluation

In table I, the results of the proposed algorithm are given. The method has been tested on a dataset composed by 120 iris images from 30 different individuals, made available to the MICHE II participants on the contest web site. More details on the performance evaluation can be found on the competition web site <sup>5</sup>.

The performance obtained on the IP5 vs. IP5 set, i.e. only images captured by the Apple iPhone 5 device are considered, achieved a Area Under ROC Curve (AUC) value of 0.98 that, on a challenging database as the MICHE DB, is a pretty good result, considering that only the information coming from the iris is used by the proposed algorithm.

The performance drops to an AUC of 0.80 when evaluating the algorithm on a test set composed by pictures captured by the Samsung Galaxy S4 device (GS4 vs. GS4).

In figure 8 the Cumulative Match Characteristic curve (CMC) and the Receiver Operating Characteristic curve (ROC) obtained in the All vs. All evaluation are shown.

### D. Computational time

The performance evaluation discussed in the previous section, has been obtained by comparing 60 Probe images against 60 Gallery images, for a total of 3600 comparisons. We performed the test on a machine with following characteristics:

<sup>5</sup>[http://biplab.unisa.it/MICHE\\_Contest\\_ICPR2016/index.php](http://biplab.unisa.it/MICHE_Contest_ICPR2016/index.php)

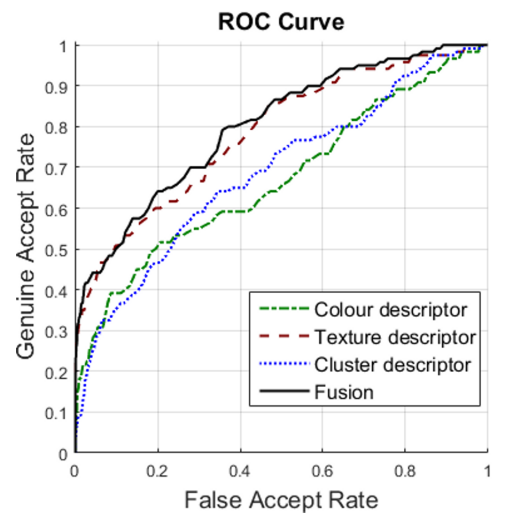
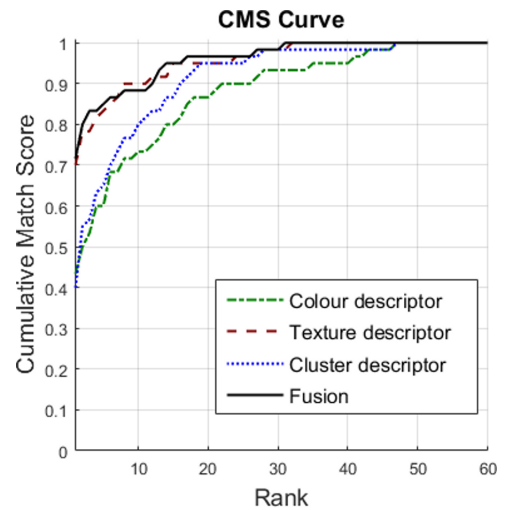


Fig. 8. CMC and ROC curve obtained from the evaluation of the proposed algorithm on the test set employed for MICHE II performance evaluation (All vs. All).

TABLE I  
PERFORMANCE EVALUATION IN TERMS OF RECOGNITION RATE (RR) AND AREA UNDER ROC CURVE (AUC).

ALL vs ALL		GS4 vs GS4		IP5 vs IP5	
RR	AUC	RR	AUC	RR	AUC
0.73	0.80	0.67	0.89	0.87	0.98

- DELL R610

- Processor: 2 x Intel(R) Xeon(R) CPU L5640 @ 2.27GHz (6 cores);
- RAM: 32GB;

The total computational time is of about 355", for an average computational time for a single comparison of about 0.0986".

#### IV. CONCLUSION

In this paper we have presented a novel and simple approach for iris recognition based on the combination of three classifiers describing different aspects of the iris, namely the colour, the texture, and the features of the clusters (colour spots) characterizing the iris. The performances have been assessed on a subset of the MICHE DB composed by pictures captured by two smartphones, namely the Apple i Phone 5 (IP5) and the Samsung Galaxy S4 (GS4). Additional experiments have been carried out by further splitting the test set in two sets, one containing only pictures captured by the IP5 and the other one containing photos acquired by the GS4.

The performances achieved on the subset composed by pictures captured by the IP5 device are pretty good, with an AUC of 0.98. The fact that the performances drop on the GS4 images, need further investigations and can maybe be due to the fact that those pictures are somehow more challenging because of the device characteristics or because of the different image resolution (IP5 images in MICHE have a rather lower resolution with respect to GS4 ones). The same behaviour has been observed in the performances of almost all the algorithm submitted to the MICHE II challenge and reported on the challenge web site<sup>6</sup>. However, a more exhaustive testing on a wider set of images is required to analyse this aspect in more details.

#### REFERENCES

- [1] H. Proena and L. A. Alexandre, "The NICE.I: Noisy Iris Challenge Evaluation Part I", IEEE First International Conference on Biometrics: Theory, Applications and Systems, BTAS 2007, pp. 1-4.
- [2] M. De Marsico, M. Nappi, and D. Riccio, "Noisy Iris Recognition Integrated Scheme", Pattern Recognition Letters 33(8): 1006-1011 (2012)
- [3] M. De Marsico, C. Galdi, M. Nappi, and D. Riccio, "FIRME: face and iris recognition for mobile engagement", Image Vis. Comput. (2014) Volume 32, Issue 12, December 2014, pp. 1161-1172.
- [4] S. Barra, A. Casanova, F. Narducci, and S. Ricciardi, "Ubiquitous iris recognition by means of mobile devices", Pattern Recognition Letters, vol. 57, pp. 66-73, 2015
- [5] A. F. Abate, M. Frucci, C. Galdi, and D. Riccio, "BIRD: watershed Based IRis Detection for mobile devices", Pattern Recognition Letters, Volume 57, 1 May 2015, pp. 43-51.
- [6] J. G. Daugman, "How iris recognition works", IEEE Trans. Circuits Syst. Video Technol., vol. 14, no. 1, pp. 2130, Jan. 2004
- [7] M. De Marsico, M. Nappi, D. Riccio, and H. Wechsler, "Mobile Iris Challenge Evaluation - MICHE - I, Biometric iris dataset and protocols", Pattern Recognition Letters, Volume 57, 1 May 2015, pp. 17-23.
- [8] J. M. Buenaposada and L. Baumela, "Variations of Grey World for face tracking", Image Processing and Communications, 7(3-4):51-62, 2001.
- [9] M. Haindl and M. Krupicka, "Unsupervised detection of non-iris occlusions", Pattern Recognition Letters, Volume 57, 1 May 2015, Pages 60-65, ISSN 0167-8655, <http://dx.doi.org/10.1016/j.patrec.2015.02.012>.

<sup>6</sup>[http://biplab.unisa.it/MICHE\\_Contest\\_ICPR2016/finalrank.php](http://biplab.unisa.it/MICHE_Contest_ICPR2016/finalrank.php)